

# Quantum Entanglement in the S=1/2 Spin Ladder with Ring Exchange

Jun-Liang Song, Shi-Jian Gu, and Hai-Qing Lin

Department of Physics and Institute of Theoretical Physics,  
The Chinese University of Hong Kong, Hong Kong, China

(Dated: February 1, 2008)

In this paper we study the concurrence and the block-block entanglement in the  $S = 1/2$  spin ladder with four-spin ring exchange by the exact diagonalization method of finite cluster of spins. The relationship between the global phase diagram and the ground-state entanglement is investigated. It is shown that the block-block entanglement of different block size and geometry manifests richer information of the system. We find that the extremal point of the two-site block-block entanglement on the rung locates a transition point exactly due to  $SU(4)$  symmetry at this point. The scaling behavior of the block-block entanglement is discussed. Our results suggest that the block-block entanglement can be used as a convenient marker of quantum phase transition in some complex spin systems.

PACS numbers: 03.67.Mn, 05.70.Jk, 75.10.Jm

## I. INTRODUCTION

Entanglement, as one of the most intriguing feature of quantum mechanics [1], has become a subject of intense interest in recent years. Besides being recognized as a kind of crucial resource of quantum computing and quantum information process [2, 3], it has also provided new perspectives in problems of various many-body systems. Particularly, the entanglement can well characterize the features of quantum phase transition (QPT) [4]. Many works [5, 6, 7, 8, 9, 10, 11, 12, 13, 14, 15, 16, 17, 18, 19] have been devoted to understanding the relationship between QPT and the entanglement in different systems. It has been observed that quantum phase transitions are signaled by critical behaviors of concurrence [20], a measure of entanglement for two-qubit system, in a number of spin models [5, 6, 7, 8, 9]. For example, it was reported that the first derivative of the concurrence diverges at the transition point in the one-dimensional transverse field Ising model [5], while the concurrence shows cusp-like behavior around the critical point in some 2D and 3D spin models [7]. Besides the concurrence, the block-block entanglement [21] which involves more system degree of freedom was introduced [12, 13, 14]. Especially in fermionic systems in which the concurrence is usually not applicable, the block-block entanglement can also manifest interesting properties, such as logarithmic divergence in the critical region, in a certain class of models [13, 14].

However, most of the previous works were restricted within the models with two-body interaction, the entanglement in the models with three-body or four-body interactions [22] is less investigated and understood. In fact a system with multi-body interaction is important both in quantum information theory and condensed matter physics. It was pointed out that a small cluster of spins with three-body or four-body interactions such as the four-spin ring exchange could be used for quantum computing [23, 24]. Moreover, four-spin ring exchange exists in many physical systems and plays an important role in understanding the magnetism in several 2D quantum

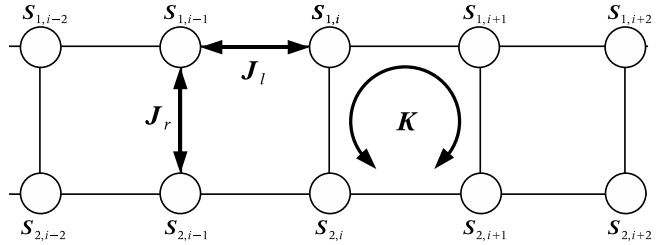


FIG. 1: A sketch of spin ladder with ring exchange.

solids such as solid  $^3\text{He}$  [25] and Wigner Crystals [26]. Therefore, it is of importance to study the properties of the entanglement in those spin systems with multi-body interactions.

In this paper, we consider a two-legged  $S = 1/2$  ladder with additional four-spin ring exchange. The system has a very rich phase diagram [27, 28, 29, 30] with many exotic phases. We investigate the concurrence and the block-block entanglement in this system, and try to relate them with the global phase diagram. The rest of the paper is organized in the following way. In section II, we introduce the model Hamiltonian and its phase diagram. In section III, we study the ground-state concurrence and discuss its relationship with the phase diagram. In section IV, we show that the two-site block-block entanglement is exactly either maximal or minimal at a QPT point. In section V, we show that the scaling behavior and some extremal point in the block-block entanglement can be used as marker of QPTs. In the final section, we summarize our results and draw conclusions.

## II. MODEL HAMILTONIAN AND PHASE DIAGRAM

The two-legged  $S = 1/2$  spin ladder with ring exchange (as shown in Fig. 1) is described by the following Hamil-

tonian

$$\begin{aligned}\hat{H} = & J_r \sum_i \hat{S}_{1,i} \hat{S}_{2,i} + J_l \sum_i \left( \hat{S}_{1,i} \hat{S}_{1,i+1} + \hat{S}_{2,i} \hat{S}_{2,i+1} \right) \\ & + K \sum_i \left( \hat{P}_{i,i+1} + \hat{P}_{i,i+1}^{-1} \right),\end{aligned}\quad (1)$$

where  $i = 1, \dots, N/2$ ,  $N$  is the total number of spins,  $\hat{S}_{1,i}$  ( $\hat{S}_{2,i}$ ) is  $1/2$  spin operator on the upper (lower) leg at the  $i$ th position, and  $J_l$  ( $J_r$ ) is the bilinear exchange constants along the legs (on the rung) and  $K$  is the coupling constant of four-spin cyclic exchange interaction  $\hat{P}$ .  $\hat{P}_{i,i+1}(\hat{P}_{i,i+1}^{-1})$  rotates the four spin in the  $i$ th plaquette clockwise (counterclockwise), i.e.

$$\hat{P} \begin{vmatrix} a & b \\ d & c \end{vmatrix} = \begin{vmatrix} d & a \\ c & b \end{vmatrix} \quad \text{and} \quad \hat{P}^{-1} \begin{vmatrix} a & b \\ d & c \end{vmatrix} = \begin{vmatrix} b & c \\ a & d \end{vmatrix},$$

and they can be decomposed in terms of spin operator involving bilinear and bi-quadratic terms,

$$\begin{aligned}\hat{P} + \hat{P}^{-1} = & \frac{1}{4} + \hat{S}_a \hat{S}_b + \hat{S}_b \hat{S}_c + \hat{S}_c \hat{S}_d + \hat{S}_d \hat{S}_a \\ & + \hat{S}_a \hat{S}_c + \hat{S}_b \hat{S}_d \\ & + 4 \left[ \left( \hat{S}_a \hat{S}_b \right) \left( \hat{S}_c \hat{S}_d \right) + \left( \hat{S}_a \hat{S}_d \right) \left( \hat{S}_b \hat{S}_c \right) \right. \\ & \left. - \left( \hat{S}_a \hat{S}_c \right) \left( \hat{S}_b \hat{S}_d \right) \right].\end{aligned}\quad (2)$$

Following the convention in Ref. [28], we set  $J_l = J_r = \cos \theta$  and  $K = \sin \theta$  in the following calculation.

Previous studies [28] suggested a rich phase diagram in the parameter space of  $\theta$  shown in the Fig. 2. There are typically six phases (regions): the rung singlet phase, the staggered dimmer phase, scalar chirality phase, dominant vector chirality region, dominant collinear spin region and the ferromagnetic phase. Squares in Fig. 2 denote first-order phase transitions, circles denote second-order phase transitions, and the dashed line indicates a crossover boundary without a phase transition.

Using the exact diagonalization method, we obtain the ground-state concurrence and the block-block entanglement in a spin ladder up to  $N = 12 \times 2$  sites with periodical boundary conditions. Although the staggered dimmer and scalar chirality phases are  $Z_2$  symmetry breaking phase with double degeneracy in the thermodynamic limit, the ground state is unique for most values of  $\theta$  except the ferromagnetic phase in a finite-size system. We select  $S_z = 0$  state out of the  $N + 1$  fold degenerate  $S = N/2$  ferromagnetic states in the following calculation.

### III. GROUND-STATE CONCURRENCE

The entanglement between the spins at site  $i$  and site  $j$  can be measured by the concurrence [20]. Let  $\rho_{ij}$  be the reduced density matrix which is obtained by tracing out all degrees of freedom of spins except that at

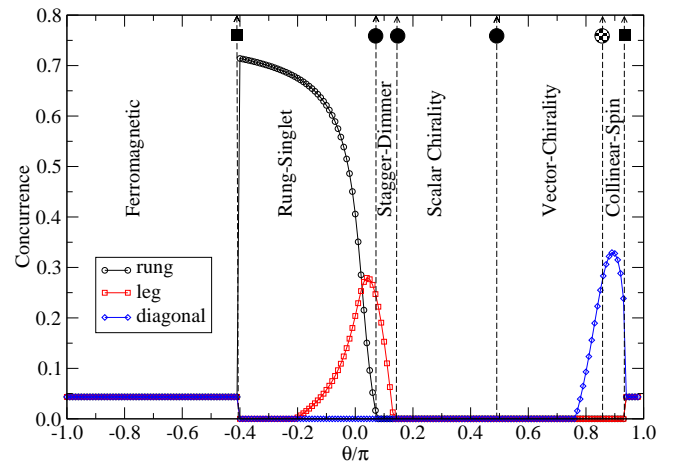


FIG. 2: (color online) The ground-state concurrence of two spins on a rung, leg, and diagonal bond as a function of  $\theta$  in  $N = 12 \times 2$  spin ladder with ring exchange. The dashed line is the boundary of different phases. The squares on these line denote a first-order phase transition, the black circle denotes a second order transition, while the shaded circle indicates a transition between two adjacent regions.

sites  $i$  and  $j$ , and  $\tilde{\rho}_{ij}$  be the spin-reversed reduced density matrix of  $\rho_{ij}$ , i.e.,  $\tilde{\rho} = (\sigma_y \otimes \sigma_y) \rho^* (\sigma_y \otimes \sigma_y)$ , where  $\sigma_y$  is the Pauli matrix. The concurrence  $C$  is given by  $C = \max(\lambda_1 - \lambda_2 - \lambda_3 - \lambda_4, 0)$ , where  $\{\lambda_i\}$  are the square roots of the eigenvalues of the matrix  $\rho \tilde{\rho}$  in descending order.  $C = 0$  means no entanglement, while  $C = 1$  the maximum entanglement such as that roots in Bell states.

In Fig. 2 we show the ground-state concurrence as a function of  $\theta$  for a  $N = 12 \times 2$  system. In the ferromagnetic phase, we can see that the concurrence on any two sites is the same and equals to  $1/(N - 1)$ . It vanishes in the thermodynamic limit ( $N \rightarrow \infty$ ). In the rung singlet phase, we can observe a rather large concurrence ( $\theta \sim 0.7\pi$ ) between the two spins on the same rung. This fact is consistent with the picture that the ground state is approximated by the product state of spin singlet on the rungs. Similarly, the concurrence of two adjacent spins on the same leg is consistent with the physical picture of staggered singlets on the leg in the staggered dimmer phase. We notice that the peak of concurrence on the leg ( $\sim 0.3$ ) is much smaller than that in the rung singlet phase ( $\sim 0.7$ ). This is because the ground state in the staggered dimmer phase is two-fold degenerate in the thermodynamic limit. Then in a finite-size system with periodic boundary conditions, the ground state is actually a superposition of these two states, thus the value of the concurrence on the leg reduce to the half of the original value. In fact if we impose boundary condition in the same way as that in Ref. [31], one of the two degenerate states will be projected out, the staggered pattern of the leg concurrence appears and the value on the dimmer leg is nearly 0.6 which is approaching to 0.7 in the

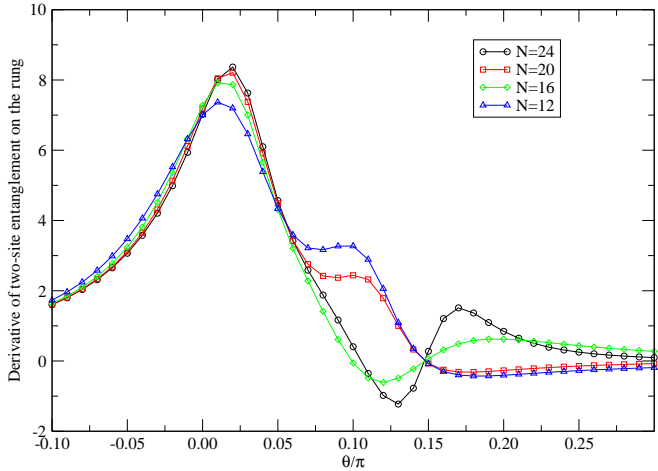


FIG. 3: (color online) The first derivative of the two-site entanglement on a rung as a function of  $\theta$ . Lines of different system sizes cross at the same point ( $\arctan(1/2)$ , 0).

rung singlet phase. In both the scalar chirality phase and dominant vector chirality phase, the concurrence of any pair of spin vanishes. However, at the cross-over region between the dominant vector chirality and dominant collinear spin region, an unexpected concurrence on the diagonal pair appears and its maximal point ( $\theta \sim 0.85\pi$ ) is roughly the crossover point between the dominant vector chirality region and dominant collinear spin region.

#### IV. TWO-SITE ENTANGLEMENT OF THE RUNG AND THE $SU(4)$ POINT

In this section and the following section, we study the block-block entanglement of various blocks in this system. The block-block entanglement is the von Neumann entropy  $E_v$  of a block of spin in the system. Precisely, it is calculated as:

$$E_v(A) = -\text{tr}(\rho_A \log_2 \rho_A), \quad (3)$$

where  $A$  is a set of sites and  $\rho_A$  is the corresponding reduced density matrix. If the whole system is in a pure state, then

$$E_v(A) = E_v(B) = -\text{tr}(\rho_B \log_2 \rho_B), \quad (4)$$

where  $B$  is the rest part of the system. Then  $E_v(A)$  or  $E_v(B)$  describes how much the block  $A$  and the rest of the system are entangled.

Compared to the concurrence, the block-block entanglement can apply to systems with much higher degrees of freedom, however, it is only meaningful when the concerning state is a pure state. In our calculation of finite-size ladders, it is found that the ground state is always non-degenerate in the region  $-0.40\pi < \theta < 0.95\pi$ . Considering the  $SU(2)$  symmetry of the Hamiltonian, the ground state's total spin is also zero in this region.

The term two-site entanglement of a rung means that the von Neumann entropy is calculated from the reduced density matrix of two spins on the same rung. In Fig. 3 we show the first derivative of the entanglement as a function of  $\theta$  for different system size. From the figure, we observe that the first derivative of the entanglement on a rung reaches zero exactly at  $\theta = \arctan(1/2) \sim 0.148\pi$  which is the QPT point between the staggered dimer phase and the scalar chirality phase. We find that this result is independent of system size. Recently, it was pointed out that, at this QPT point the system restores  $SU(4)$  symmetry[29]. Precisely speaking, at  $\theta_c = \arctan(1/2)$ , the Hamiltonian commutes with the following operator [29]:

$$\hat{T} = \sum_i \hat{S}_{1,i} \cdot \hat{S}_{2,i}. \quad (5)$$

We will show that the expectation value of  $\hat{T}$  is maximal or minimal exactly at  $\theta = \theta_c$  due to the above symmetry.

As discussed above, we can assume the ground state  $|\psi_0\rangle$  is non-degenerate around  $\theta_c$ , which implies  $|\psi_0\rangle$  is also the eigenstate of  $\hat{T}$  at  $\theta_c$ , thus we have  $\hat{T}|\psi_0\rangle = \lambda_t|\psi_0\rangle$  in which  $\lambda_t$  is some real number. Then the first derivative of  $\langle \hat{T} \rangle$  with  $\theta$  at  $\theta_c$  is

$$\begin{aligned} \frac{d}{d\theta} \langle \psi_0 | \hat{T} | \psi_0 \rangle &= \langle \frac{d\psi_0}{d\theta} | \hat{T} | \psi_0 \rangle + \langle \psi_0 | \hat{T} | \frac{d\psi_0}{d\theta} \rangle \\ &+ \langle \psi_0 | \frac{d\hat{T}}{d\theta} | \psi_0 \rangle \\ &= \lambda_t \langle \frac{d\psi_0}{d\theta} | \psi_0 \rangle + \lambda_t^* \langle \psi_0 | \frac{d\psi_0}{d\theta} \rangle + 0 \\ &= \lambda_t \frac{d}{d\theta} \langle \psi_0 | \psi_0 \rangle \\ &= 0. \end{aligned} \quad (6)$$

Therefore, the expectation value of  $\hat{T}$  reaches local maximum or minimum at  $\theta_c$ . Since the ground state has  $(k_x, k_y) = (0, 0)$ , the system is invariant under translation along the leg, so  $\langle \hat{S}_{1,i} \cdot \hat{S}_{2,i} \rangle = \langle \hat{S}_{1,j} \cdot \hat{S}_{2,j} \rangle$  (for any two site  $i$  and  $j$  in the ladder) is either maximal or minimal at  $\theta_c$ .

Next we show that there is one-to-one correspondence between the  $\langle \hat{S}_{1,i} \cdot \hat{S}_{2,i} \rangle$  and the two-site entanglement on the rung in the vicinity of  $\theta_c$ . Let  $\rho_{ij}$  be the reduced density matrix of spins of sites  $i$  and  $j$  of the ground state. In the basis  $\{|\downarrow\downarrow\rangle, |\uparrow\downarrow\rangle, |\uparrow\uparrow\rangle, |\downarrow\uparrow\rangle\}$ ,  $\rho_{ij}$  has the following form due to the  $U(1)$  symmetry of the ground state in the concerning region( $0.1\pi < \theta < 0.2\pi$ ):

$$\rho_{ij} = \begin{pmatrix} u^+ & 0 & 0 & 0 \\ 0 & w_1 & z^* & 0 \\ 0 & z & w_2 & 0 \\ 0 & 0 & 0 & u^- \end{pmatrix}. \quad (8)$$

Moreover, in the vicinity of  $\theta = \theta_c$ , the ground state is unique and its total spin  $S = 0$ , which implies the ground

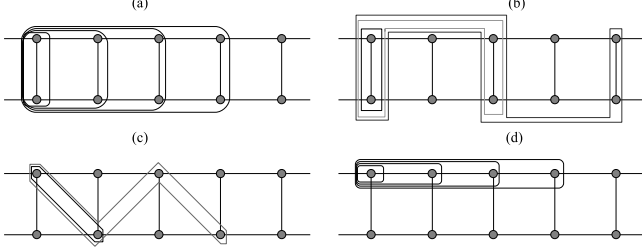


FIG. 4: Four choices of increasing the block size: (a) is the single block, (b) is the stripe block, (c) is the zigzag block, (d) is one-leg block.

state is also invariant under any rotations. Particularly,  $\rho_{ij}$  is invariant under the rotation around the  $x$  axis:

$$[\sigma_i^x + \sigma_j^x, \rho_{ij}] = 0. \quad (9)$$

From Eq. (9), and the condition  $\text{tr}\rho = 1$ , we have

$$u^+ = u^- = \frac{1+2z}{4}, \quad w_1 = w_2 = \frac{1-2z}{4}, \quad (10)$$

$$z = z^*, \quad \langle \hat{S}_{1,i} \cdot \hat{S}_{2,i} \rangle = -\frac{3z}{2}, \quad (11)$$

Then the block-block entanglement on the rung  $E_r$  is

$$E_r = -3u^+ \log_2 u^+ - (w_1 - z) \log_2 (w_1 - z). \quad (12)$$

From the above equations it is clear that this extremal behavior of two-site entanglement on the rung is directly related to the  $SU(4)$  symmetry.

## V. SCALING BEHAVIOR OF THE BLOCK-BLOCK ENTANGLEMENT

In this section, we focus on the scaling behavior of the block-block entanglement, namely how the block-block entanglement behaves as the block size changes. Unlike the case in the one dimensional chain, the ladder geometry has provided us many choices of how to select the block's shape and how to increase the block size. As shown in Fig. 4, we choose four different ways to increase the block size.

First, we notice that in the ferromagnetic phase, the value of the block-block entanglement depends only on the size of the block. It is independent of the block geometry. This is because any two sites in this state is essentially equivalent as we have already seen in Sec. III. In fact an explicit expression of block-block entanglement as a function of block size  $l$  can be obtained in the following calculation.

The ferromagnetic  $S_{tot}^z = \sum_i S_i^z = 0$  state  $\psi_{FM}(S_{tot}^z = 0)$  could be obtained by applying lowering operator on the  $\psi_{FM}(S_{tot}^z = N/2)$   $N/2$  times.

$$|\phi_{FM}(0)\rangle = \frac{\left(\sum_{i=1}^N \hat{S}_i^-\right)^{\frac{N}{2}}}{\sqrt{\left(\frac{N}{2}\right)!}} \underbrace{|\uparrow\uparrow\uparrow\cdots\uparrow\rangle}_N, \quad (13)$$

where  $\hat{S}_i^-$  is the spin lowering operator at site  $i$  and  $N$  is the total number of sites. In the basis  $\{|\downarrow\downarrow\rangle, |\downarrow\uparrow\rangle, |\uparrow\downarrow\rangle, |\uparrow\uparrow\rangle\}$ , all the coefficients of  $\psi_{FM}(S_{tot}^z = 0)$  are the same:  $\sqrt{(N/2)!(N/2)!/N!}$ . The matrix element  $\rho_l(p, q)$  could be obtained explicitly:

$$\rho_l(p, q) = \begin{cases} \frac{\left(\frac{N-l}{2}\right)!\left(\frac{N}{2}\right)!\left(\frac{N}{2}\right)!}{\left(\frac{N-l}{2}-p_z\right)!\left(\frac{N-l}{2}+p_z\right)!(N)!} & \text{if } p_z = q_z \\ 0 & \text{if } p_z \neq q_z \end{cases}. \quad (14)$$

In the above expression,  $\rho_l$  is reduced density matrix of the block consisting of  $l$  spins (we assume  $l \leq N/2$ ),  $p$  and  $q$  are the column and row index of  $\rho_l$ ,  $p_z$  and  $q_z$  are the corresponding  $S_{tot}^z$  number.

After diagonalizing this matrix, there are only  $l+1$  nonzero eigenvalues  $\lambda_{p_z}$  with  $p_z = -l/2, -l/2+1, \dots, l/2$ . Then the block-block entanglement can be obtained as:

$$\begin{aligned} \lambda_{p_z} &= \frac{(l)!\left(\frac{N-l}{2}\right)!\left(\frac{N}{2}\right)!\left(\frac{N}{2}\right)!}{\left(\frac{l}{2}-p_z\right)!\left(\frac{l}{2}+p_z\right)!\left(\frac{N-l}{2}-p_z\right)!\left(\frac{N-l}{2}+p_z\right)!(N)!}, \\ E_v(l) &= \sum_{p_z=-l/2}^{l/2} -\lambda_{p_z} \log_2 \lambda_{p_z}. \end{aligned} \quad (15)$$

When  $l$  and  $N$  are large, the summation in Eq. (15) can be replaced by an integral, and the function  $\lambda_{p_z}$  can be approximated by the Gaussian Distribution. Thus we can approximate  $E_v l$  by the following expression:

$$E_v(l) \sim -\frac{1}{2} \log_2 \left( \frac{1}{l} + \frac{1}{N-l} \right) + \frac{1}{2} \log_2 \left( \frac{\pi e}{2} \right), \quad (16)$$

which suggests that  $E_v(l)$  diverges logarithmically as the size  $l$  increases.

Secondly, in Fig. 5(a), in the most region of rung singlet phase, the block-block entanglement converges to some finite value quickly, while in 5(b)–(d), it is almost proportional to the block size. Since the ground state is approximately the rung singlet product state, the block-block entanglement is proportional to the number of bonds cross the boundary of the block such as in case (c) and (d). In case (b), the situation is different since the number of bonds cross the boundary of block is finite, thus the short-ranged correlations between the rungs plays important role in (b) and explains this proportionality.

Next, in Fig. 5(b)–(d), we find that some local extreme points of the block-block entanglement may be the QPT points. Previous studies[28, 29] suggested that the transition point between the rung singlet and staggered

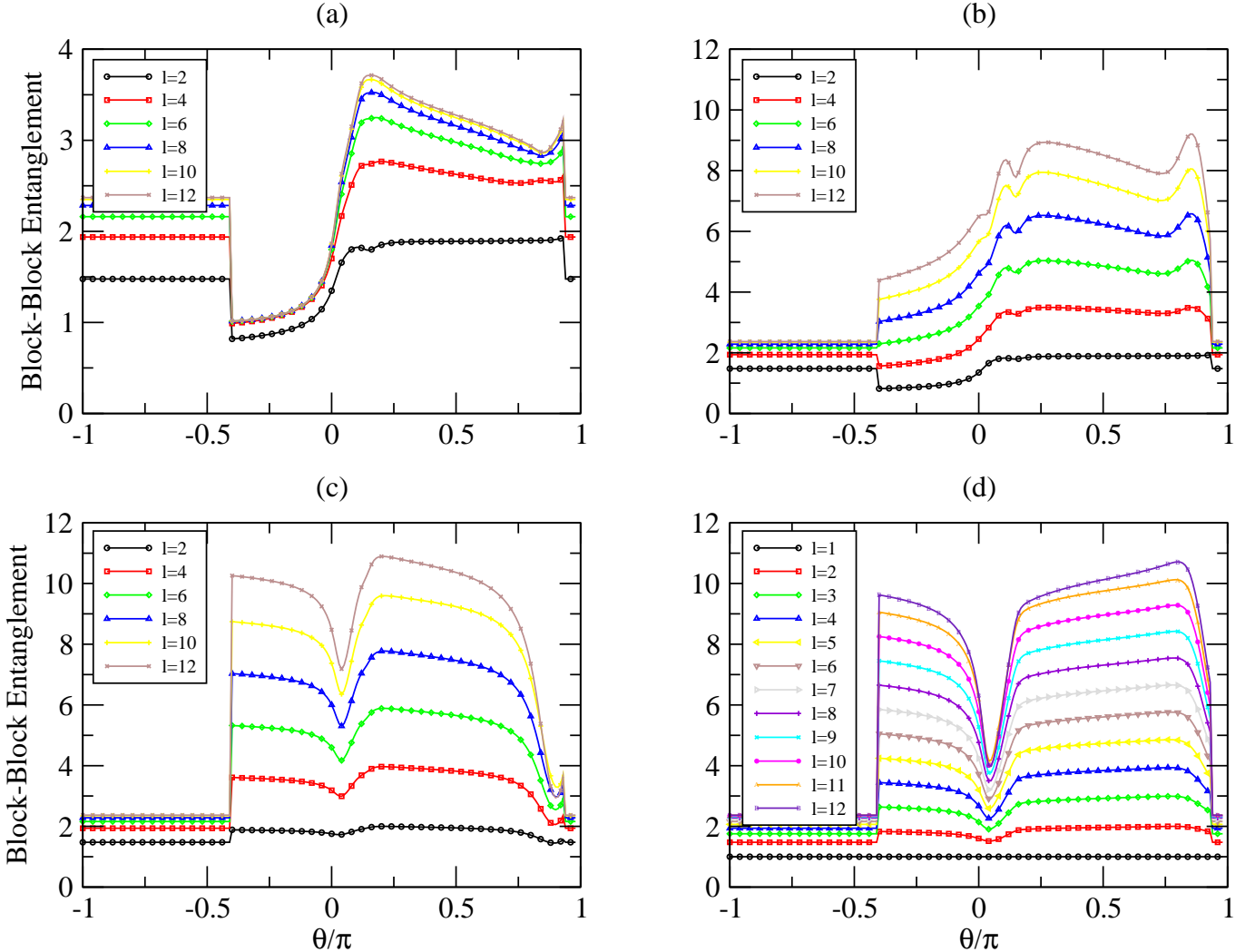


FIG. 5: (color online) The block-block entanglement of different block size  $l$  as a function of  $\theta$  in  $N = 12 \times 2$  ladder. The geometry of the blocks in (a)(b)(c)(d) are specified in Fig. 4(a)(b)(c)(d).

dimmer to be  $0.06\pi \sim 0.08\pi$  which is quite near the local maximum point  $0.07\pi$  in (b), local minimum  $0.05\pi$  in (c) and (d). The transition point between the staggered dimmer and scalar chirality phase is exactly  $0.148\pi$  which is also near one minimal point  $0.14\pi$  in (b). As for the crossover point between the dominant vector chirality region and the dominant collinear spin region, (b)-(d) all suggest the value  $\sim 0.85\pi$  which is coincidence with the value obtained in previous works[28].

In general, the scaling behavior of the above four choices of blocks could be categorized into two kinds, Fig. 5(a) and (b)-(d). In (a), the number of ladder bonds across the boundary between two blocks is a finite value which equals to 4 independent of the block size, while in (b)-(d), the number is proportional to the block size  $l$ . In the latter case, the short-ranged correlation across the boundary bonds is main contribution to the block-block entanglement, thus the block-block entanglement is always proportional to the size of the block as we have

seen in Fig. 4. In the former case, the main contribution to the block-block entanglement comes from the long-range correlation between the sites in the block and the sites outside the blocks. It is expected that around the QPT point, in the former case the scaling behavior changes abruptly, e.g. from convergence to finite value to divergence logarithmically, while in the latter case, there may exist extremal point of the block-block entanglement which is an indication of QPT.

## VI. SUMMARY AND ACKNOWLEDGMENT

In summary, we have studied the concurrence and the block-block entanglement in the ground state of the  $S = 1/2$  spin ladder with ring exchange. In both the rung singlet and staggered dimer phase, the behaviors of the ground-state concurrence are consistent with the corresponding dominant configurations. The extremal

point of the two-site block-block entanglement coincide with the QPT point due to the  $SU(4)$  symmetry, and such a symmetry is obviously independent of the system size. We have also investigated the scaling behavior of the block-block entanglement for different block geometry and block size. We have identified three kinds of typical scaling behavior in this model, namely increasing the size of block, the block-block entanglement (a) converges to some finite value, (b) diverges logarithmically

with size, (c) diverges proportional with the size. However, as we can see that, there's no signature of the QPT between the scalar chirality phase and dominant vector chirality phase.

This work is supported by the Earmarked Grant for Research from the Research Grants Council of HKSAR, China (Project CUHK N\_CUHK204/05 and HKU\_3/05C).

---

[1] A. Einstein and B. Podolsky and N. Rosen, Phys. Rev. **47**, 777 (1935).

[2] C. H. Bennett and D. P. Divincenzo, Nature **404**, 247 (2000).

[3] M. A. Nielsen and I. L. Chuang, *Quantum Computation and Quantum Information*, (Cambridge University Press, 2000).

[4] S. Sachdev, *Quantum Phase Transitions*, (Cambridge University Press, 2000).

[5] A. Osterloh, Luigi Amico, G. Falci, Rosario Fazio, Nature **416**, 608 (2002).

[6] T. J. Osborne and M.A. Nielsen, Phys. Rev. A **66**, 032110(2002).

[7] S. J. Gu, H. Q. Lin, and Y. Q. Li, Phys. Rev. A **68**, 042330 (2003); S. J. Gu, G. S. Tian, H. Q. Lin, Phys. Rev. A **71**, 052322 (2005).

[8] R. G. Unanyan and C. Ionescu and M. Fleischhauer, Phys. Rev. A **72**, 022326 (2005).

[9] J. Vidal, quant-ph/0603108.

[10] S. Yi and H. Pu, Phys. Rev. A **73**, 023602 (2006).

[11] X. F. Qian, T. Shi, Y. Li, Z. Song, and C. P. Sun, Phys. Rev. A **72**, 012333 (2005).

[12] S. J. Gu and G. S. Tian and H. Q. Lin, New J. Phys. **8**, 61 (2006).

[13] G. Vidal, J. I. Latorre, E. Rico, and A. Kitaev, Phys. Rev. Lett. **90**, 227902 (2003).

[14] V. E. Korepin, Phys. Rev. Lett. **92**, 096402 (2004).

[15] S. J. Gu, S. S. Deng, Y. Q. Li, H. Q. Lin, Phys. Rev. Lett. **93**, 086402 (2004); S. S. Deng, S. J. Gu, and H. Q. Lin, Phys. Rev. B in press.

[16] Daniel Larsson and Henrik Johannesson, Phys. Rev. Lett **95**, 196406 (2005).

[17] Ö. Legeza and J. Sólyom, Phys. Rev. Lett. **96**, 116401 (2006).

[18] Alberto Anfossi, Paolo Giorda, Arianna Montorsi, and Fabio Traversa, Phys. Rev. Lett. **95**, 056402 (2005); Alberto Anfossi, Cristian Degli Esposti Boschi, Arianna Montorsi, and Fabio Ortolani, Phys. Rev. B **73**, 085113 (2006).

[19] L. Campos Venuti, C. Degli Esposti Boschi, M. Roncaglia, and A. Scaramucci, Phys. Rev. A **73**, 010303(R) (2006).

[20] W. K. Wootters, Phys. Rev. Lett. **80**, 2245 (1998).

[21] K. Audenaert, J. Eisert, M. B. Plenio, and R. F. Werner, Phys. Rev. A **66**, 042327 (2002).

[22] Indrani Bose and Amit Tribedi, Phys. Rev. A **72**, 022314 (2005).

[23] Ari Mizel and Daniel A. Lidar, Phys. Rev. Lett. **92**, 077903 (2004).

[24] V. W. Scarola and K. Park and S. Das Sarma, Phys. Rev. Lett. **93**, 120503 (2004).

[25] M. Roger and C. Bäuerle and Yu. M. Bunkov and A. S. Chen and H. Godfrin, Phys. Rev. Lett. **80**, 1308 (1998).

[26] Tohru Okamoto and Shinji Kawaji, Phys. Rev. B **57**, 9097 (1998).

[27] M. Müller and T. Vekua and H. J. Mikeska, Phys. Rev. B, **66**, 134423 (2002).

[28] A. Läuchli and G. Schmid and M. Troyer, Phys. Rev. B **67**, 100409(R) (2003).

[29] Toshiya Hikihara and Tsutomu Momoi and Xiao Hu, Phys. Rev. Lett. **90**, 087204 (2003).

[30] S. Brehmer and H. J. Mikeska and M. Müller and N. Nagaosa and S. Uchida, Phys. Rev. B. **60**, 329 (1999).

[31] T. Hakobyan and J. H. Hetherington and M. Roger, Phys. Rev. B, **63**, 144433 (2001).